

GENERATION OF LINEAR WAVES WITH BOTTOM WAVE MAKERS IN A FLUME: AN EFFICIENT WAY TO ABSORB REFLECTED WAVES

Minh Thang Tran, Sejong University, tranmthang08@gmail.com
 Jae-Sang Jung, Korea Rural Community Corporation, fangon@ekr.or.kr
 Changhoon Lee, Sejong University, clee@sejong.ac.kr
 Yong-Sung Park, Seoul National University, dryspark@snu.ac.kr

INTRODUCTION

When waves are generated in a flume by the conventional piston or flap wave maker, waves reflected from structures will arrive at the wave maker and experience re-reflection. These re-reflected waves will propagate to the structures so that the target wave energy cannot be accurately obtained. Since 1980s, methods of internally generating waves inside a computational domain and putting sponge layers at the domain end have been developed in numerical modelling. Internally generated waves will propagate both directions from the wave generation zone and waves reflected from the structures will pass through the wave generation zone without any reflection by the wave maker and be absorbed in the sponge layers. Using the idea of internal generation of waves, Jung et al. (2018) developed bottom wave makers in a flume which have paddles moving up and down from the bottom (see also Lu et al. (2017)). In this study, following Jung et al.'s (2018) techniques, we numerically develop both rectangular and triangular bottom wave makers in a flume using the analytical method and the extended mild-slope equations.

DEVELOPMENT OF ANALYTICAL SOLUTIONS AND EXTENDED MILD-SLOPE EQUATIONS

We obtained analytical solutions of generation of linear waves using the Laplace and Fourier transform techniques. The water depth can be expressed as

$$h = h_0 - \Delta h(x)\Lambda(t) \quad (1)$$

where $\Delta h(x)$ is the space-dependent wave maker amplitude and $\Lambda(t)$ is the time-dependent wave maker elevation at a position. We consider both rectangular and triangular bottom wave makers (see Fig. 1). Analytical solutions of water surface elevations ζ for rectangular and triangular bottom wave makers are obtained, respectively, as

$$\zeta(x, t) = \frac{\Delta h_0 \omega_0}{\pi} \int_{-\infty}^{\infty} \frac{\sin\left(\frac{kb}{2}\right) e^{-ikx}}{k \cosh kh_0 (gk \tanh kh - \omega_0^2)} \left[\sqrt{gk \tanh kh} \sin(\sqrt{gk \tanh kh} t) - \omega_0 \sin(\omega_0 t) \right] dk \quad (2)$$

$$\zeta(x, t) = \frac{4\Delta h_0 \omega_0}{\pi b} \int_{-\infty}^{\infty} \frac{\left[\sin\left(\frac{kb}{4}\right)\right]^2 e^{-ikx}}{k^2 \cosh kh_0 (gk \tanh kh - \omega_0^2)} \left[\sqrt{gk \tanh kh} \sin(\sqrt{gk \tanh kh} t) - \omega_0 \sin(\omega_0 t) \right] dk \quad (3)$$

where b is the wave maker length and ω_0 is the angular frequency of the bottom movement and k is the wave number.

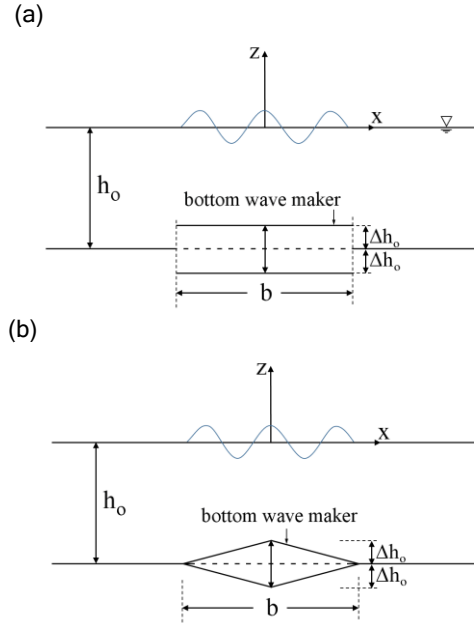


Fig. 1. Definition sketch for solution of wave generation with two types of bottom wave makers. (a) rectangular bottom wave maker, (b) triangular bottom wave maker.

We also developed a numerical model of the extended mild-slope equations for linear waves on bottom varying in time using the Lagrangian formulation given by

$$\frac{\partial \tilde{\phi}}{\partial t} = -g\zeta \quad (4)$$

$$\frac{\partial \zeta}{\partial t} = -\nabla \cdot \left(\frac{C_p C_g}{g} \nabla \tilde{\phi} \right) + \frac{\omega^2 - k^2 C_p C_g}{g} \tilde{\phi} - \frac{1}{\cosh kh} \frac{\partial h}{\partial t} \quad (5)$$

where $\tilde{\phi}$ is the velocity potential at mean water level and where C_p and C_g are the phase speed and the group velocity, respectively.

NUMERICAL EXPERIMENTS

We first compared the results of the analytical method and the extended mild-slope model and found that both the analytical solutions and the numerical solutions of generated linear regular waves agree with each other in whole water depths. Water surface elevations generated by the rectangular bottom wave maker becomes more different from linear sinusoidal waves because the rectangular bottom

movement elevations are different from sinusoidal shape. It was also observed that the bottom wave makers are more efficient in generating waves in shallow water while the conventional piston and flap wave makers are more efficient in deep water (Lu et al., 2017).

After simulating the extended mild-slope model, we found that waves reflected from structures pass over the bottom wave maker with very little reflection and are absorbed in the sponge layer located at the domain end. Fig. 2 shows incident wave surface elevations at $t=72T$ and total wave surface elevations at $t=71.1T, 71.2T, \dots, 72T$ for the triangular bottom wave maker with ratio of wave maker length to wavelength $b/\lambda = 0.5$ and the ratio of water depth to wavelength $h_0/\lambda = 1/40$. The standing wave heights on the right side are two times as the incident wave heights because of full reflection at the right boundary. The total waves on the left side are composed of the incident waves and the transmitting waves passing over the wave maker. The total wave heights are almost constant in space because wave reflection by the wave maker is negligibly small which shows that waves pass over the bottom wave maker with very little reflection.

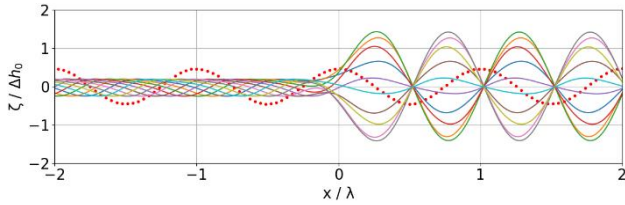


Fig. 2. Surface elevations of incident waves (dot) and surface elevations of total waves (solid line).

Next, a ratio of generated wave bottom movement amplitude $a/\Delta h_0$ versus the ratio of wave maker width to wavelength b/λ for the rectangular bottom wave maker and the triangular bottom wave maker was considered, respectively. The analytical solutions and the extended mild-slope equation solutions are almost equal to each other. The rectangular bottom wave maker yields higher wave amplitudes than the triangular bottom wave maker because the rectangular wave maker moves water volume two times the triangular bottom wave maker. In shallow water, generated wave amplitudes are high because the water surface is directly affected by the bottom movement. In deep water, however, generated wave amplitudes are negligibly low because the water surface is little affected by the bottom movement.

Using the information of the ratio of generated wave amplitude to bottom movement amplitude, we successfully generated bi-chromatic and irregular waves with the extended mild-slope model. First, we simulate two monochromatic waves with slightly different frequencies of f_1 and f_2 in a depth given by

$$h(x, t) = \begin{cases} h_0 - \Delta h_0 \left(1 - \frac{2|x|}{b}\right) \sin(2\pi f_i t), & |x| \leq \frac{b}{2} \\ h_0, & |x| > \frac{b}{2} \end{cases} \quad (i = 1, 2) \quad (8)$$

and then linearly superpose the two solutions. Second, we simulate bi-chromatic waves with a representative mean frequency $\bar{f} (= 0.5(f_1 + f_2))$ in a depth given by

$$h(x, t) = \begin{cases} h_0 - \Delta h_0 \left(1 - \frac{2|x|}{b}\right) [\sin(2\pi f_1 t) + \sin(2\pi f_2 t)], & |x| \leq \frac{b}{2} \\ h_0, & |x| > \frac{b}{2} \end{cases} \quad (9)$$

Then, we compared the two solutions, i.e., the linearly superposed solution for two monochromatic waves and the solution for representative waves, which are almost exactly the same. In order to generate linear irregular waves with the triangular bottom wave maker, we specify the water depth as

$$h(x, t) = \begin{cases} h_0 - \sum_i \Delta h_{0i} \left(1 - \frac{2|x|}{b}\right) \sin(2\pi f_i t + \varepsilon_i), & |x| \leq \frac{b}{2} \\ h_0, & |x| > \frac{b}{2} \end{cases} \quad (10)$$

where $\Delta h_{0i} = a_i/c_i = \sqrt{2S(f_i)\Delta f}/c_i$, $c_i = a_i/\Delta h_{0i}$ is the ratio of generated wave amplitude a_i to bottom movement amplitude Δh_{0i} , and $S(f_i)$ is the frequency spectrum.

Fig. 3 shows time series of surface elevations of generated waves at a position of $x = 7\lambda_p$ which are irregular both in frequency and amplitude. In Fig. 4, power spectrum of water surface elevations measured at a position of $x = 7\lambda_p$ is almost the same as the target value. The bottom wave makers can be used to efficiently generate linear long waves in a flume without disturbances of reflected waves from structures.

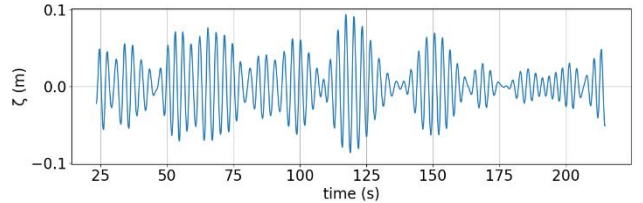


Fig. 3. Time series of surface elevations at $x = 7\lambda_p$.

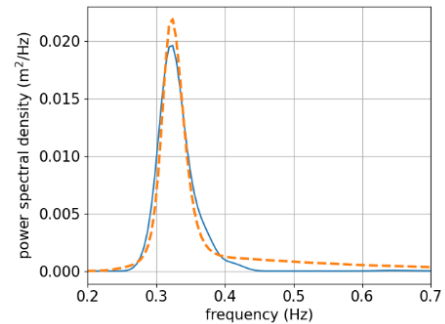


Fig. 4. Power spectrum of surface elevations at $x = 7\lambda_p$ (solid line: measured data, dashed line: target).

ACKNOWLEDGEMENTS

This research was supported by a grant (code: 22CTAP-C164367-02) from the Technology Advancement Research Program (TARP) funded by the Ministry of Land, Infrastructure and Transport of Korean government.

REFERENCE

- Jung, J.-S., Lee, C. and Pham, V.K. (2018): A study of performance of bottom moving wave maker: Comparison of analytical and numerical solutions, Proc. Korean Association of Ocean Science and Technology Societies, Jeju, Korea, pp. 54-57 (in Korean).
- Lu, H., Park, Y.S. and Cho, Y.-S. (2017): Modelling of long waves generated by bottom-tilting wave maker, Coastal Eng. Vol. 122, pp. 1-9.